Neuro-Oncology 13(12):1308–1323, 2011.
doi:10.1093/neuonc/nor134
Advance Access publication September 8, 2011

Thymus-derived rather than tumor-induced regulatory T cells predominate in brain tumors

Derek A. Wainwright, Sadhak Sengupta, Yu Han, and Maciej S. Lesniak

The Brain Tumor Center, The University of Chicago, Chicago

Glioblastoma multiforme (GBM) is a highly malignant brain tumor with an average survival time of 15 months. Previously, we and others demonstrated that CD4$^+$FoxP3$^+$ regulatory T cells (Tregs) infiltrate human GBM as well as mouse models that recapitulate malignant brain tumors. However, whether brain tumor-resident Tregs are thymus-derived natural Tregs (nTregs) or induced Tregs (iTregs), by the conversion of conventional CD4$^+$ T cells, has not been established. To investigate this question, we utilized the i.c. implanted GL261 cell-based orthotopic mouse model, the RasB8 transgenic astrocytoma mouse model, and a human GBM tissue microarray. We demonstrate that Tregs in brain tumors are predominantly thymus derived, since thymectomy, prior to i.c. GL261 cell implantation, significantly decreased the level of Tregs in mice with brain tumors. Accordingly, most Tregs in human GBM and mouse brain tumors expressed the nTreg transcription factor, Helios. Interestingly, a significant effect of the brain tumor microenvironment on Treg lineage programming was observed, based on higher levels of brain tumor-resident Tregs expressing glucocorticoid-induced tumor necrosis factor receptor and CD103 and lower levels of Tregs expressing CD62L and CD45RB compared with peripheral Tregs. Furthermore, there was a higher level of nTregs in brain tumors that expressed the proliferative marker Ki67 compared with iTregs and conventional CD4$^+$ T cells. Our study demonstrates that future Treg-depleting therapies should aim to selectively target systemic rather than intratumoral nTregs in brain tumor-specific immunotherapeutic strategies.

Keywords: brain cancer, CD4, CD25, FoxP3, GBM, glioblastoma, glioma, RasB8, regulatory T cells, Tregs.

Received June 6, 2011; accepted July 15, 2011.

Corresponding Author: Maciej S. Lesniak, MD, The Brain Tumor Center, The University of Chicago, 5841 S. Maryland Ave, MC 3026, Chicago, IL 60637 (mlesniak@surgery.bsd.uchicago.edu).

Glioma is a type of brain tumor that arises from a cell with glial lineage in the CNS. Of the different glioma subtypes, glioblastoma multiforme (GBM) is highly malignant, with poor treatment options. Following initial diagnosis, most GBM patients undergo debulking surgery, and when also treated with radiotherapy, they can expect an average lifespan of 12.1 months, which can be extended to 14.6 months if they are treated with both radiotherapy and the chemotherapeutic drug temozolomide.[1] Thus, additional treatment strategies are needed to address the poor median survival of patients with GBM. Accordingly, we and others have recently demonstrated that immunomodulation may be a useful therapeutic tool.[2–5] Our laboratory was one of the first to discover that immunosuppressive CD4$^+$FoxP3$^+$CD25$^+$ regulatory T cells (Tregs) infiltrate GBM and mouse models that recapitulate malignant brain tumors,[6,7] which has been independently verified.[8,9] Furthermore, Treg-depletion studies have suggested that these cells play a negative role in brain tumor progression, ultimately decreasing overall lifespan.[4] It has also been suggested that in the future, Treg-depletion strategies should become more specific. This is based on recent studies showing that while current methods inhibit the progression of and/or eliminate GBM tumors in mouse models, they can also inhibit clonal expansion of tumor antigen-specific T cells when utilized combinatorially with immunotherapy.[10]

Tregs play a critical role in preventing autoimmunity through the immunosuppressive cell surface ligands glucocorticoid-induced tumor necrosis factor receptor (GITR) and cytotoxic T-lymphocyte antigen (CTLA)-4,[11,12] as well as through the production of the immunosuppressive cytokines transforming growth factor-beta (TGF-β) and interleukin-10,[13] and can be divided into thymus-derived and peripherally inducible subsets. As the name implies, thymus-derived natural Tregs (nTregs) develop in the thymus,[14,15] express FoxP3,[16] maintain peripheral tolerance, and emerge from the thymus with T-cell receptors specific to self-antigens.[17] Alternatively, peripherally induced Tregs (iTregs) arise outside of the thymus by conversion of conventional CD4$^+$FoxP3$^-$ T cells into CD4$^+$FoxP3$^+$

© The Author(s) 2011. Published by Oxford University Press on behalf of the Society for Neuro-Oncology.
All rights reserved. For permissions, please e-mail: journals.permissions@oup.com.

Tregs when coexposed to antigen-presenting cells and high levels of TGF-β or suboptimal stimulation of T-cell receptors.[18,19]

Determining the absolute levels of nTregs and iTregs during immune responses has historically been difficult, since no clear markers have been available, resulting in indirect means of quantification.[20] However, recent work has demonstrated that nTregs, but not iTregs, express the Ikaros family transcription factor, Helios.[21] Thus, it is now possible to directly quantify the level of thymus-derived Tregs in brain tumors. This is an important consideration when designing Treg-depleting/-inactivating therapies, since human nTregs appear to have greater lineage stability compared with iTregs with regard to interconversion into other T-cell helper types.[21] If nTregs are the principal residents in brain tumors, depleting them systemically may be beneficial, whereas if conventional $CD4^+$ T cells are converted into iTregs inside the brain tumor, depleting them intratumorally or decreasing the factors that promote iTreg development will be preferred. Therefore, this study determined whether thymus-derived, tumor-induced, or both subtypes of Tregs are present in the brains of mice using both orthotopic and transgenic mouse brain tumor models as well as in human GBM.

Materials and Methods

Mice, Procedures, and Murine Glioma Cell Line

C57BL/6 mice were obtained from Jackson Laboratories, maintained in our laboratory, and used at ages between 6 and 9 weeks. Hemizygous transgenic RasB8 mice were obtained from Abjihit Guha (Hospital for Sick Children), endogenously expressing a single allele of oncogenic V^{12}HA-ras and maintained in our laboratory. RasB8 mice were maintained on the CD1 background. Mice exhibiting one or several of the following signs were considered symptomatic: abnormal fur coat, hunched posture, lack of normal motion/activity, and weight loss. All mice were provided autoclaved food pellets and water ad libitum. All surgical procedures were completed in accordance with National Institutes of Health guidelines on the care and use of laboratory animals for research purposes. Thymectomy procedures were conducted on the mice at Jackson Laboratories at 4 weeks of age and 3 weeks prior to murine glioma (GL261)-cell implantation. Systemic CD25 monoclonal antibody (mAb) treatment was performed with a single i.p. injection of 1-mg anti-CD25 (PC61; Fitch Monoclonal Antibody Facility) 3 days prior to GL261 cell implantation. Mice were sacrificed by cervical dislocation. GL261 cells were cultured in Dulbecco's modified Eagle's medium supplemented with 10% fetal calf serum as well as streptomycin (100 mg/mL) and penicillin (100 U/mL) at 37°C in a humidified atmosphere of 95% air/5% CO_2. All cell culture products were purchased from Gibco Invitrogen.

Mouse Orthotopic Intracranial Injection Model

Mice were anesthetized with an i.p. injection of 0.1-mL stock solution containing ketamine HCl (25 mg/mL), xylazine (2.5 mg/mL), and 14.25% ethyl alcohol (diluted 1:3 in 0.9% NaCl). For the stereotactic i.c. injection, the surgical site was shaved and prepared with 70% ethyl alcohol. A midline incision was made and a 1-mm-diameter right parietal burr hole was drilled, centered 2 mm posterior to the coronal suture and 2 mm lateral to the sagittal suture. Mice were placed in a stereotactic frame and 2.5 μL of saline or 4×10^5 GL261 cells in 2.5 μL saline was i.c. injected with a 26-gauge needle at a depth of 3 mm. The needle was removed and the skin was sutured with 4-0 nylon thread.

Flow Cytometry

Single cell suspensions were made from brain, thymus, cervical draining lymph node (dLN), or spleen by mashing cells through a sterile 70-μM nylon mesh cell strainer (Fisher Scientific), using the rubber end of a 3-mL syringe, into ice-cold phosphate buffered saline (PBS; Gibco). Red blood cells were removed by treatment with ACK (ammonium chloride/potassium) Lysing Buffer (Lonza) for 4 min on ice. Cells were stained in PBS + 1% bovine serum albumin (Sigma-Aldrich) and stained with anti-CD4-PB (pacific blue) or anti-CD4-PE (phycoerythrin)-Cy7 (RM4-5; Ebioscience), anti-CD45RB-PE (16A; Becton Dickinson [BD]), anti-CD62L-FITC (fluorescein isothiocyanate) (MEL-14; BD), CD127-FITC (A7R34; Ebioscience), GITR-APC (allophycocyanin) (DTA-1; Ebioscience), and CD103-FITC (M290; BD) for 30 min on ice. Cells were then permeabilized and fixed overnight at 4°C using the Mouse Regulatory T Cell Staining Kit (Ebioscience) according to manufacturer's instructions and stained with anti-FoxP3-APC (FJK-16s; Ebioscience), anti-Helios-alexa fluor 488 (22F6; Biolegend), and anti-Ki67 (Abcam) for 30 min on ice, followed by donkey anti-rabbit-PB (Invitrogen). Cellular frequency was determined by the LSR II flow cyotometer (BD) and Flowjo analysis software (TreeStar).

Histology and Immunofluorescence

Brain, spleen, thymus, and cervical dLNs were taken from mice i.c. injected with saline or GL261 cells at 3 weeks postoperative (WPO) and were flash frozen and sectioned at 8 μm intervals. Sections were postfixed with 4% paraformaldehyde, blocked for endogenous biotin for 5 min (1% H_2O_2 in PBS), and blocked for nonspecific staining with 10% bovine serum albumin (Sigma-Aldrich) in PBS for 1 h. Sections of mouse tissue were incubated with anti-CD4-alexa fluor 488 (GK1.5, 1:50; Ebioscience), anti-Helios-alexa fluor 647 (22F6, 1:50; Biolegend), and biotinylated anti-FoxP3 (FJK-16S, 1:250; Ebioscience) in PBS at 4°C overnight. Sections were washed extensively and incubated with

streptavidin-alexa fluor 555 (1:500) for 2.5 h. Following extensive washing in PBS, sections were covered with Ultra Cruz mounting media (Santa Cruz). Images of antibody-stained sections were captured using the Sp5 Tandem Scanner 2 photon confocal microscope (Leica Microsystems) running LAS AF software (Leica Microsystems) using the argon, orange NeHe, and red NeHe laser lines. Fluorescent images were captured using the 20× or 63× objectives. Additionally, 3 WPO mouse brains with brain tumors were stained with hematoxylin and eosin (H&E) to visualize tumor size and i.c. localization. Images of H&E staining were photographed using the rolling objective of the Macroscope (MVX10; Olympus) running cellSens software.

GBM Tissue Array

The brain GBM tissue array (BS17018; US Biomax) was deparaffinized in xylene and rehydrated through a descending-strength ethanol series before being rinsed in water. The slide was heated in a sodium citrate buffer (10 mM sodium citrate, 0.05% Tween-20, pH 6.0) at 97°C for 40 min and cooled at room temperature for 20 min. Sections were rinsed in PBS, serum- and biotin-blocked as described above, and incubated overnight with biotinylated anti-FoxP3 (PCH101, 1:250; Ebioscience) and anti-Helios-alexa fluor 488 (22F6, 1:50; Biolegend). Sections were washed extensively and incubated with streptavidin-alexa fluor 555 for 2.5 h. Following extensive washing in PBS, sections were covered with Ultra Cruz mounting media with 4',6-diamidino-2-phenylindole (DAPI; Santa Cruz). For each GBM specimen, 3 separate and randomly selected areas demonstrating FoxP3 staining were chosen, with the third area captured for quantification. Photomicrographs of antibody-stained GBM sections were captured using the Sp5 Tandem Scanner 2 photon confocal microscope (Leica Microsystems) running LAS AF software (Leica Microsystems) using the orange NeHe and red NeHe laser lines. Positive signals were counted in each field and their total number determined. To be counted, the Helios and/or FoxP3 immunofluorescent signal was required to be >5 μm and ≤ 10 μm. All other signals were considered to be nonspecific. Fluorescent images were captured using the 63× objective. For control staining, a separate brain tumor tissue array was treated as described above, incubated with biotinylated rat immunoglobulin (Ig)G_{2A} (1:250; Ebioscience) and hamster IgG-alexa fluor 488 (HTK888, 1:250; Biolegend) and counterstained with DAPI.

Statistical Analysis

Survival curves were calculated according to Kaplan–Meier. Overall survival is defined as the time from injection of GL261 cells to day 76 of the time course. The *P*-value was obtained by log-rank statistical analysis and was considered significant when $P \leq .05$. For non-survival curves, data are presented as ±SEMs and were analyzed by 2-way analysis of variance (ANOVA), 1-way ANOVA, or the 2-tailed Student's *t*-test, and $P \leq .05$ was considered significant. Post-hoc analyses were performed using Bonferonni's, Newman–Keuls, and/or Fieller's method for multicomparison procedures. All analyses were performed using GraphPad Prism version 4.00 (GraphPad Software).

Results

Thymectomy and/or CD25 mAb Decreases Brain-Resident Treg Levels in an Orthotopic Mouse Brain Tumor Model

To investigate the overall contribution of nTregs in mouse brain tumor, we selectively thymectomized mice, with or without administration of the Treg-depleting CD25 mAb, prior to i.c. implantation of the murine GL261 cell line or saline (Supplementary Figs. S1–S3). A low level of $CD4^+FoxP3^+$ Tregs was observed in the brain of all groups at 1 WPO (Fig. 1A). However, by 3 WPO, only mice with brain tumors had a detectable Treg presence. Accordingly, the 3 WPO level of $CD4^+FoxP3^+$ Tregs in brain with tumors from unthymectomized mice that had been i.p. injected with saline was $2.0 \pm 0.38\%$, which was higher than $0.67 \pm 0.11\%$ for unthymectomized mice i.p. injected with CD25 mAb ($P < .01$), as well as $0.62 \pm 0.15\%$ or $0.43 \pm 0.05\%$ for thymectomized mice i.p. injected with saline or CD25 mAb, respectively ($P < .01$). Importantly, the combination of thymectomy and CD25 mAb in mice with brain tumors at 3 WPO decreased the total Treg level by $78\% \pm 11\%$ compared with mice with brain tumors that were left unthymectomized and not treated with CD25 mAb. These data indicate that by removing the origin of nTreg development via thymectomy, Treg levels significantly decreased in mouse brain tumors. This effect was recapitulated in mice that were systemically treated with CD25 mAb.

Fig. 1. Thymectomy (Tx) and/or systemic CD25 mAb decreases the level of $CD4^+FoxP3^+$ Tregs in an orthotopic GL261 cell-based mouse brain tumor model. Mice were ± thymectomized at 4 weeks of age (WOA), i.p. injected at 6.6 WOA with saline or CD25 mAb, and i.c. injected at 7 WOA with saline or 4×10^5 GL261 cells and sacrificed at 8 WOA (1 week postoperative [WPO]) or 11 WOA (3 WPO) (Supplementary Fig. S1A). Representative flow cytometry was analyzed for CD4 and FoxP3 and gated on forward scatter (FSC)/side scatter (SSC) for leukocytes from the (A) brain, (B) thymus, (C) cervical draining lymph nodes (dLNs), and (D) inguinal nondraining lymph nodes at 1 and 3 WPO. Bar graphs in figures A–D are shown as mean ± SEM and are representative of 2 independent experiments ($n = 3$–5 per group). $^*P < .05$, $^{**}P < .01$. ND, not detectable.

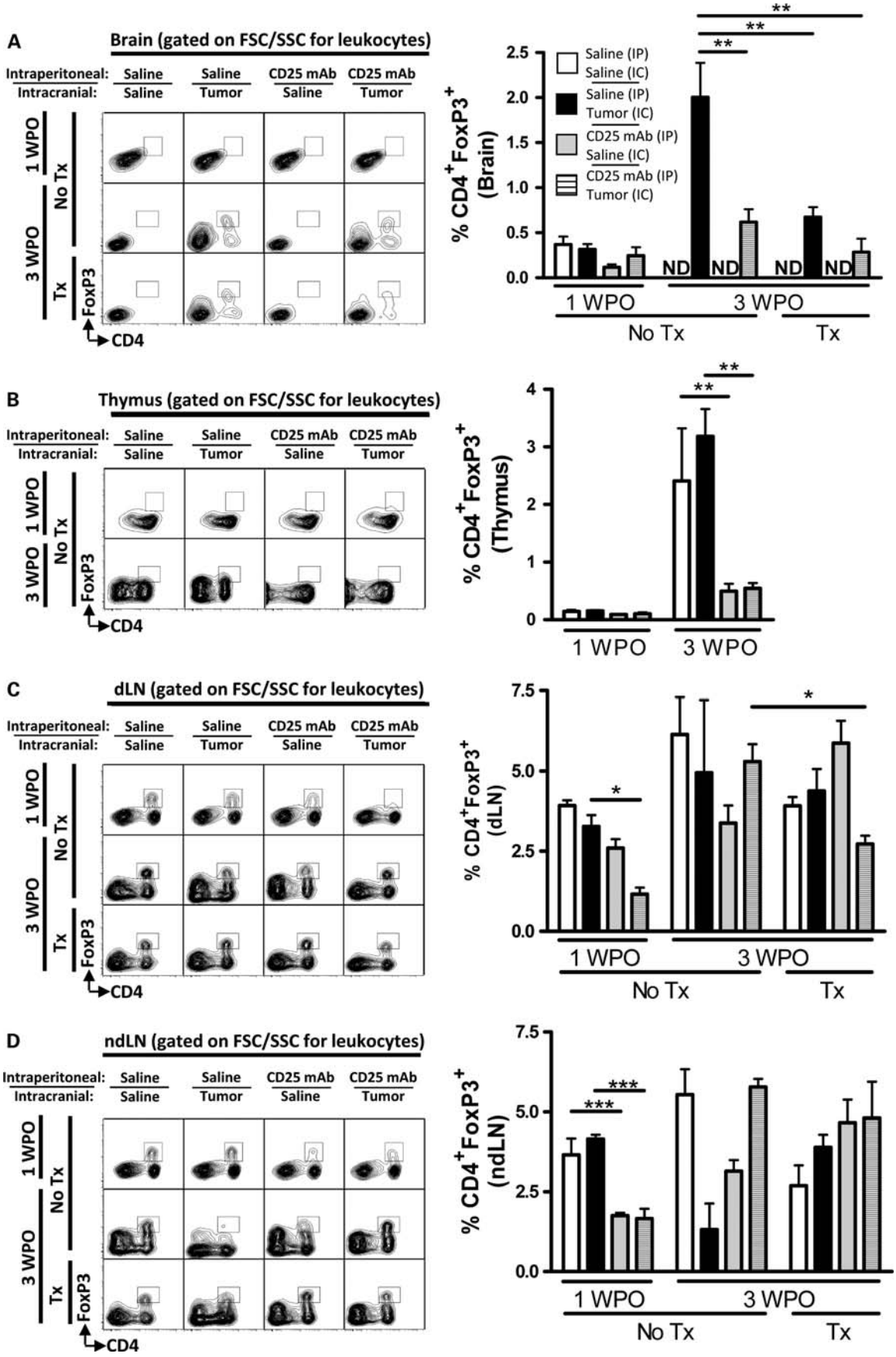
A
Brain (gated on FSC/SSC for leukocytes)
Intraperitoneal: Saline Saline CD25 mAb CD25 mAb
Intracranial: Saline Tumor Saline Tumor
1 WPO
3 WPO
No Tx
Tx
FoxP3
CD4
Saline (IP) Saline (IC)
Saline (IP) Tumor (IC)
CD25 mAb (IP) Saline (IC)
CD25 mAb (IP) Tumor (IC)
% CD4+FoxP3+ (Brain)
ND
1 WPO
3 WPO
No Tx
Tx
B
Thymus (gated on FSC/SSC for leukocytes)
% CD4+FoxP3+ (Thymus)
C
dLN (gated on FSC/SSC for leukocytes)
% CD4+FoxP3+ (dLN)
D
ndLN (gated on FSC/SSC for leukocytes)
% CD4+FoxP3+ (ndLN)

Collectively, the data suggest that nTregs significantly contribute to the overall presence of Tregs in brain tumors.

To determine whether the systemic effects of the Treg-depleting antibody, CD25 mAb, were directed toward the thymus, the levels of thymic-resident Tregs were quantified at 1 and 3 WPO under the conditions previously described (Supplementary Fig. S1). The level of Tregs at 1 WPO in mouse thymus increased in mice with or without brain tumors from $0.15 \pm 0.03\%$ and $0.15 \pm 0.03\%$ to $3.2 \pm 0.48\%$ and $2.4 \pm 0.92\%$, respectively, by 3 WPO ($P < .01$) (Fig. 1B). In contrast, the level of Tregs at 1 WPO in mice administered the Treg-depleting CD25 mAb with or without brain tumors was not significantly changed by 3 WPO. Collectively, these data suggest that the Treg-depleting CD25 mAb effectively targets thymus-derived Tregs for clearance, regardless of the presence or absence of brain tumor. Furthermore, combining the observations that (1) CD25 mAb decreases the level of Tregs in the thymus and (2) CD25 mAb decreases the level of Tregs in brain tumors, the data collectively support the hypothesis that brain-resident Tregs are predominantly populated by thymus-derived cells and helps to explain why combining thymectomy with CD25 mAb does not significantly change Treg levels in mouse brain tumors. However, since we saw such a significant impact of CD25 mAb on thymus-derived Tregs, we wondered what these effects in combination with thymectomy would be in other peripheral lymphoid organs, such as cervical dLNs.

To determine the effects of thymectomy, CD25 mAb, and brain tumor on the level of Tregs in the cervical dLN, the level of Tregs was analyzed at 1 and 3 WPO under the conditions previously described (Supplementary Fig. S1). At 1 WPO, the level of Tregs in dLN of unthymectomized mice with brain tumors i.p. injected with saline had a level of $CD4^+FoxP3^+$ Tregs of $3.3 \pm 0.36\%$, which decreased to $1.2 \pm 0.20\%$ when mice were treated with the CD25 mAb ($P < .05$) (Fig. 1C). Interestingly, thymectomy decreased the level of Tregs in the dLN of mice with brain tumors i.p. injected with CD25 mAb compared with unthymectomized mice ($P < .05$). Collectively, these data indicate that the effects of CD25 mAb in normal mice with brain tumors are transient. However, when combined with thymectomy at a later time, the effects of CD25 mAb appear to amplify the Treg decrease in tumor dLNs. Furthermore, combining the observations that (1) thymectomy decreases the level of Tregs in the dLN of mice with brain tumors treated with CD25 mAb and (2) thymectomy decreases the level of Tregs in brain tumors of mice treated with CD25 mAb, the data collectively support the hypothesis that nTregs first transit to the dLN after thymic emigration and before infiltration into the brain tumor. However, if this normal trafficking response was specific to the brain tumor and not simply a response to the combined effects of thymectomy and CD25 mAb treatment in lymph nodes, then one could hypothesize that the same level of Treg decrease would not occur in nondraining lymph nodes (ndLNs) under the same conditions.

To determine the effects of thymectomy, CD25 mAb, and brain tumor on the level of Tregs in inguinal ndLNs, the level of Tregs was analyzed at 1 and 3 WPO under the conditions previously described (Supplementary Fig. S1). Tregs at 1 WPO in ndLN of unthymectomized mice i.p. injected with or without saline or with brain tumor had a level of $CD4^+FoxP3^+$ Tregs of $3.7 \pm 0.51\%$ and $4.2 \pm 0.13\%$, respectively, which decreased to $1.8 \pm 0.08\%$ and $1.7 \pm 0.30\%$, respectively, when mice were treated with CD25 mAb ($P < .001$) (Fig. 1D). However, a similar effect was not recapitulated at 3 WPO. Furthermore, unlike in dLN, the combined effects of thymectomy and CD25 mAb treatment failed to decrease Treg levels in mice with brain tumors at 3 WPO compared with unthymectomized mice. Combining the observations that (1) thymectomy decreases the level of Tregs in the dLN of mice with brain tumors treated with CD25 mAb and (2) thymectomy has no effect on the level of Tregs in ndLN of mice with brain tumors treated with CD25 mAb, the data collectively support the hypothesis that nTregs first transit to the dLN after thymic emigration and prior to infiltration of the brain tumor.

CD25 mAb Requires the Thymus to Maximally Extend Lifespan in an Orthotopic Mouse Brain Tumor Model

Since our previous data demonstrated that thymectomy and/or CD25 mAb results in a maximal depletion of Tregs in the mouse brain tumor, we hypothesized that these treatments would have additive effects in increasing lifespan in a mouse brain tumor model. To address whether thymus-derived Tregs affect the lifespan in a GL261 cell-based mouse brain tumor model, mice were monitored for time of death over a course of 76 days and assessed for the effects of i.c. implantation, thymectomy, and Treg-depleting CD25 mAb (Supplementary Fig. S1). All control mice that received an i.c. injection of saline survived the surgical procedure to experimental completion (Fig. 2). In contrast, none of the unthymectomized mice with brain tumors i.p. injected with saline survived to experimental completion, with a median survival of 32 days. Interestingly, 10% of the thymectomized mice with brain tumors that were i.p. injected with saline survived, with a median survival of 35.5 days. Likewise, 8.3% of thymectomized mice with brain tumors i.p. injected with CD25 mAb survived, with a median survival of 38.5 days. In contrast, CD25 mAb treatment in unthymectomized mice with brain tumors resulted in a 46% survival rate and a median survival of 71 days, which was significantly increased when compared with unthymectomized mice i.p. injected with saline ($P < .001$). These data confirm previous observations from our laboratory indicating that the CD25 Treg-depleting mAb significantly increases survival in a mouse brain tumor model compared with mice not treated with CD25 mAb.[4] Also, in combination with Figure 1, these data show that while Treg levels are decreased by thymectomy in mouse brain tumors, there is little overall benefit to survival.

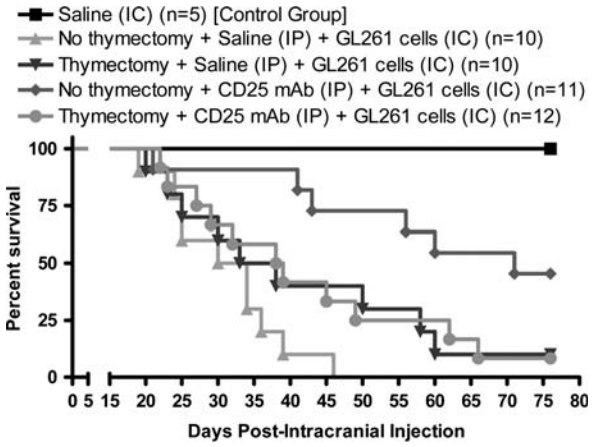

Fig. 2. Thymectomy and CD25 mAb differentially affect lifespan in an orthotopic GL261 cell-based mouse brain tumor model. Mice were ± thymectomized at 4 weeks of age (WOA), i.p. injected at 6.6 WOA with saline or CD25 mAb, and i.c. injected at 7 WOA with 4×10^5 GL261 cells (Supplementary Fig. S1A). The Kaplan–Meier curve represents mouse survival times over a course of 76 days. The control group received an i.c. injection of saline alone ($n = 5$). The remaining 4 groups ($n = 10$–12 per group) received 1 or more of the following: thymectomy; an i.p. injection of saline or CD25 mAb; and an i.c. injection of 4×10^5 GL261 cells.

Helios-Expressing Tregs Predominate in an Orthotopic Mouse Brain Tumor Model

To confirm the previous suggestion that nTregs significantly contribute to the brain tumor-resident Treg population, as well as to measure the exact level of thymus-derived Tregs, the level of $CD4^+FoxP3^+$ Tregs that express the transcription factor, Helios, was determined. The level of $CD4^+FoxP3^+$ Tregs in mouse brain tumors was 20.4 ± 3.6% and 25.1 ± 1.7% at 1 and 2 WPO, respectively, and increased to 55 ± 6.4% by 3 WPO ($P < .01$) (Fig. 3A and E; Supplementary Figs. S5 and S6). However, there were no differences in the level of Tregs in the spleen, thymus, and dLN (Fig. 3B–E). Furthermore, thymus-derived $CD4^+FoxP3^+Helios^+$ Tregs almost completely comprised the entire Treg population in mouse brain at 1, 2, and 3 WPO (Fig. 3A and F). Interestingly, the level of thymus-derived $CD4^+FoxP3^+Helios^+$ Tregs slightly decreased over the 3 WPO time frame in the spleen (Fig. 3B and F) and dLN ($P < .05$) (Fig. 3D and F), possibly suggesting an early expansion of this population, followed by a later phase of contraction. Most importantly, thymus-resident Tregs were universally Helios positive, and the levels did not change during the brain tumor time course. These data provide confirmation of the previous experimental finding that thymus-derived nTregs are the predominant population in mouse brain tumors. Furthermore, they raise the possibility that an early expansion of nTregs occurs in the spleen and dLN, since this population showed a significant contraction during later time points of brain tumor progression.

Brain-Resident nTregs Predominate in the RasB8 Spontaneously Developing Mouse Brain Tumor Model

To determine whether nTregs, rather than iTregs, constitute the majority of Tregs in brain tumors in a more physiologically relevant mouse model, we utilized symptomatic RasB8 mice, which spontaneously develop glioma.[22] In accordance with the GL261 cell-based orthotopic brain tumor mouse model, the level of $CD4^+$ T cells that express FoxP3 was highest in the brain of symptomatic RasB8 mice compared with the levels in the spleen, thymus, and dLN ($P < .001$) (Fig. 4A and B). Furthermore, the frequency of thymus-derived $CD4^+FoxP3^+Helios^+$ Tregs was 92 ± 3.4% in the brain, which was increased compared with 76 ± 4.5% and 65 ± 7.0% in the spleen and cervical dLN ($P < .05$ and $P < .001$, respectively), but not significantly different from the level found in the thymus (Fig. 4C). The proliferative marker, Ki67, was used to assess the level of proliferation in $CD4^+$ T cells.[23] In the brain and cervical dLN, the level of proliferation was highest in $CD4^+FoxP3^+Helios^+$ nTregs compared with $CD4^+FoxP3^+Helios^-$ iTregs and conventional $CD4^+$ T cells, respectively ($P < .01$) (Fig. 4D). However, there was no difference between $CD4^+$ T cell populations expressing Ki67 in the spleen or thymus. These data indicate that nTregs constitute the primary population of Tregs in mice that spontaneously develop brain tumors and that they proliferate at higher levels compared with iTregs and conventional $CD4^+$ T cells.

Anatomy of Lymphoid Tissue Changes in an Orthotopic Mouse Brain Tumor Model

To understand the microarchitectural organization of mouse brain tumor in the CNS, as well as how a primary brain tumor within the CNS can impact the peripheral lymphoid architecture, histology and immunofluorescence were performed on brain and/or spleen, thymus, and dLN in mice i.c. injected with saline or GL261 cells. The mouse brain tumor is 3–4 mm in length in the upper right hemisphere of the mouse brain at 3 WPO (Fig. 5A). Immunofluorescence indicates individual $CD4^+$ T cells in the parenchyma of the brain tumor, which are identified by the cytomembranous staining of CD4 as well as their predominant coexpression of both nuclear transcription factors, FoxP3 and Helios (Fig. 5B).

In mice i.c. injected with saline, normal splenic, thymic, and lymph node architecture is maintained (Fig. 5C). This is represented by well-defined areas of basophilic- and eosinophilic-staining red pulp in the spleen, well-defined basophilic-staining cortex and eosinophilic staining in the medulla of the thymus, and small basophilic-staining follicles in dLN. Furthermore, immunofluorescence of each tissue shows normal CD4, FoxP3, and Helios staining (Fig. 5C). In contrast, mouse brain tumors affect the normal lymphoid architecture and composition systemically, resulting in an eosinophilic-staining red pulp that constitutes the parenchyma of the spleen,

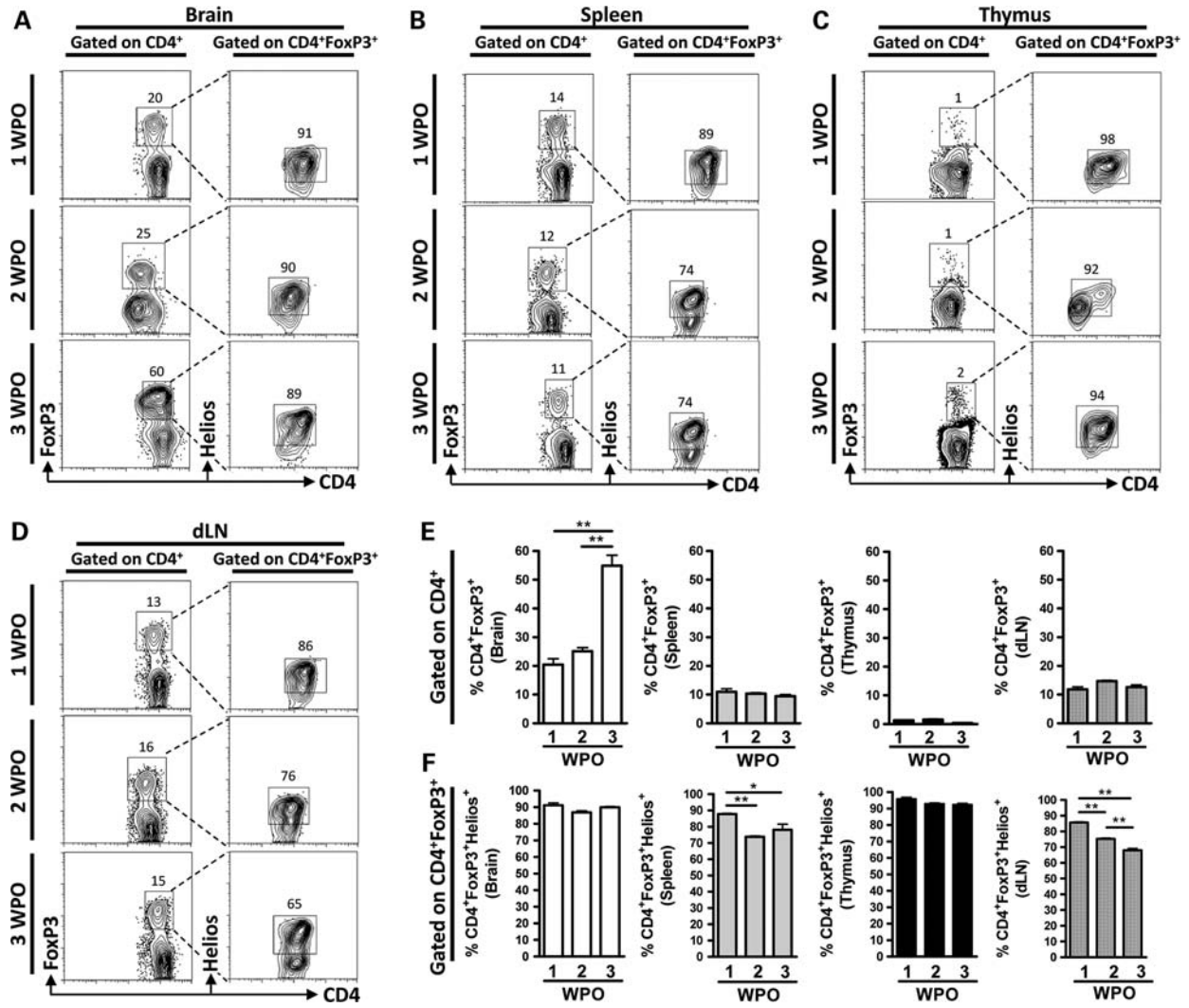

Fig. 3. $CD4^+FoxP3^+Helios^+$ thymus-derived Tregs predominate in an orthotopic GL261 cell–based mouse brain tumor model at 1, 2, and 3 weeks postoperative (WPO). Representative flow cytometry and gating strategy for determining the level of $CD4^+FoxP3^+$ Tregs and $CD4^+FoxP3^+Helios^+$ Tregs in the (A) brain, (B) spleen, (C) thymus, and (D) dLN at 1, 2, and 3 WPO ($n = 3$ per group). (Control staining was performed with Rat IgG2A for anti-FoxP3 and Hamster IgG for anti-Helios [Supplementary Figs. S5 and S6].) (E) Quantification of the gated $CD4^+FoxP3^+$ Tregs (from Fig. 3A–D) presented as bar graphs in the brain (white bars), spleen (grey bars), thymus (black bars), and dLN (hatched bars) at 1, 2, and 3 WPO ($n = 3$ per group) (gated on $CD4^+$ T cells). (F) Quantification of the gated $CD4^+FoxP3^+Helios^+$ Tregs (from Fig. 3A–D) presented as bar graphs in the brain (white bars), spleen (grey bars), thymus (black bars), and dLN (hatched bars) at 1, 2, and 3 WPO ($n = 3$ per group) (gated on $CD4^+FoxP3^+$ T cells). Data in A and B are shown as mean ± SEM and are representative of pooled data from 3 independent experiments. $^*P < .05$, $^{**}P < .01$.

the loss of a defined cortex and medulla in the thymus, and large single follicles in the dLN. Furthermore, the immunolocalization of CD4, FoxP3, and Helios demonstrate a qualitative lack of normal staining patterns in the spleen, thymus, and dLN. When directly comparing tissues from saline and GL261 cell-injected mice, $CD4^+$ T cellularity appears to be increased in the spleens of mice i.c. injected with saline compared with the spleens of mice with brain tumors. Likewise, a similar qualitative staining pattern is observed in the thymus, where all FoxP3-expressing $CD4^+$ T cells colocalize with Helios and a general lack of conventional $CD4^+$ T cells is apparent. Interestingly, the overall $CD4^+$ T cellularity in dLN from saline-injected mice appeared qualitatively decreased compared with dLN from mice with brain tumors, likely due to the ongoing T-cell response as a result of tumor-draining antigens. These data indicate that brain tumors not only recruit Tregs directly into the tumor parenchyma but also have systemic consequences for the rest of the animal. These effects are easily seen by the qualitative loss of normal microarchitecture in primary and secondary lymphoid tissues, which consequently impacts the overall $CD4^+$ T cell and/or $CD4^+FoxP3^+Helios^+$ Treg organization in each tissue.

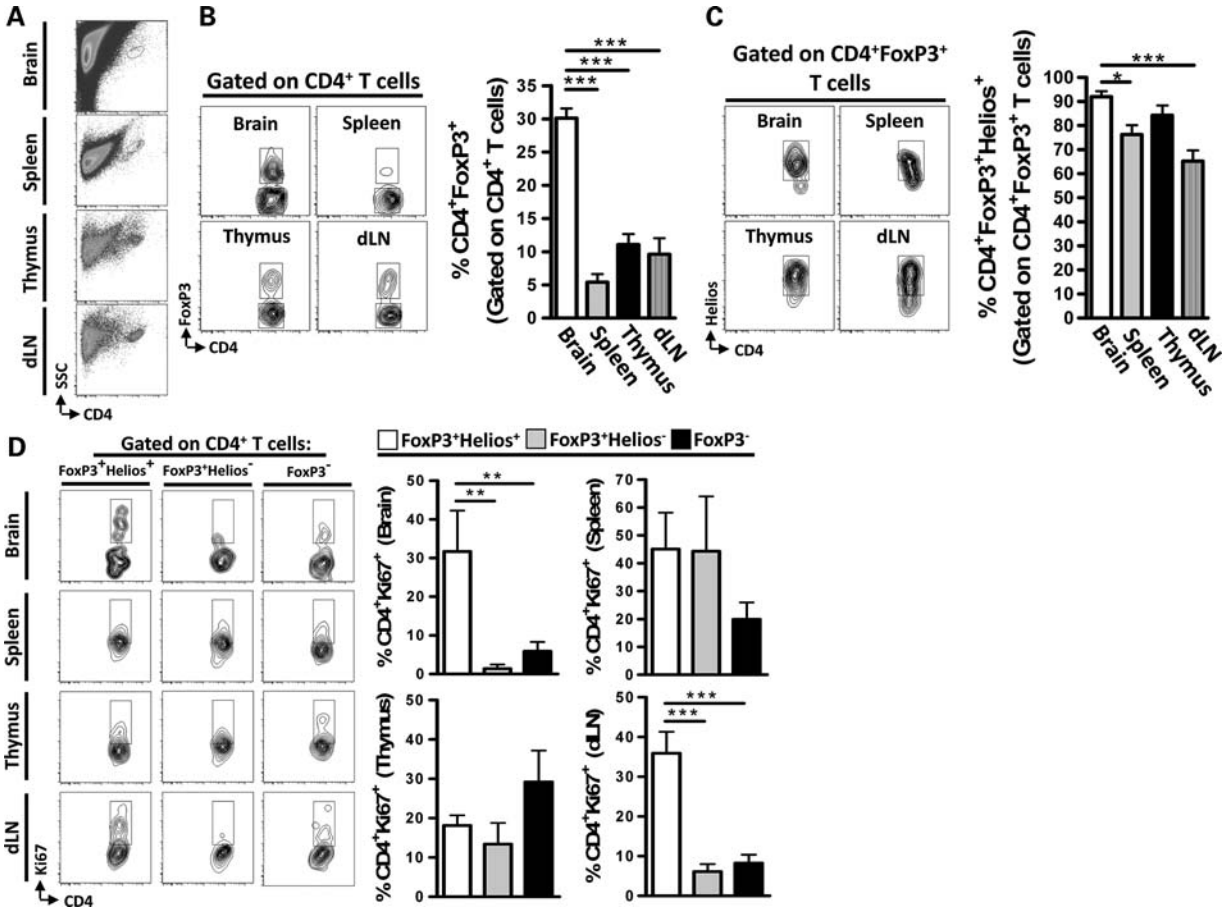

Fig. 4. Thymus-derived Tregs predominate and proliferate in the RasB8 transgenic mouse brain tumor model. (A) Representative flow cytometry demonstrating the side scatter (SSC) and CD4 marker gating strategy in the brain, spleen, thymus, and draining lymph nodes (dLNs). (B) Representative flow cytometry demonstrating the gating strategy for determining $CD4^+FoxP3^+$ T cells (gated on $CD4^+$ T cells) in the brain, spleen, thymus, and dLN. Quantification of the data from flow cytometry is shown in the bar graphs for brain (white bar), spleen (grey bar), thymus (black bar), and dLN (hatched bar) ($n = 3$ per group). (C) Representative flow cytometry demonstrating the gating strategy for determining $CD4^+FoxP3^+Helios^+$ T cells (gated on $CD4^+FoxP3^+$ T cells) in the brain, spleen, thymus, and dLN. Quantification of the data from flow cytometry is shown in the bar graphs for brain (white bar), spleen (grey bar), thymus (black bar), and dLN (hatched bar) ($n = 3$ per group). (D) Representative flow cytometry for the level of $Helios^+$ (thymus-derived) Tregs, $Helios^-$ (tumor-induced) Tregs, and $CD4^+$ conventional T cells that express the proliferation marker Ki67 ($n = 3$ per group). Data in B–D are shown as mean ± SEM and are representative of 3 independent experiments. $^*P < .05$, $^{**}P < .01$, $^{***}P < .001$.

Brain- and Spleen-Resident Tregs and Non-Tregs Differentially Express GITR, CD62L, CD103, and CD45RB in an Orthotopic Mouse Brain Tumor Model

To investigate whether the level of Tregs and conventional $CD4^+$ T cells from the brain and spleen of mice with brain tumors are similar with regard to the expression of GITR, CD62L, CD103, and CD45RB, $CD4^+FoxP3^+$, and $CD4^+FoxP3^-$ T cells were compared at 3 WPO (Fig. 6A). GITR has been shown to play a critical role in dominant immunological tolerance and to contribute to the potent immunosuppression by Tregs.[11,24] All brain-resident Tregs were GITR positive, which was decreased compared with brain-resident conventional $CD4^+$ T cells, as well as spleen-resident Tregs and conventional $CD4^+$ T cells ($P < .01$) (Fig. 6B). Interestingly, a higher level of brain-resident conventional $CD4^+$ T cells was GITR positive compared with spleen-resident non-Tregs ($P < .01$). Moreover, no difference was found when comparing the levels of $GITR^+$ spleen-resident Tregs and brain-resident conventional $CD4^+$ T cells. These data suggest that the brain tumor microenvironment not only upregulates the immunosuppressive ligand, GITR, by Tregs but also causes an upregulation of GITR by conventional $CD4^+$ T cells.

In contrast to GITR-expressing $CD4^+$ T cells, fewer brain-resident Tregs and conventional $CD4^+$ T cells were CD62L positive compared with Tregs and conventional $CD4^+$ T cells from the spleen ($P < .01$), which suggests fewer naive $CD4^+$ T cells in the brain. Furthermore, the level of spleen-resident $CD62L^+$ Tregs was decreased compared with spleen-resident non-Tregs ($P < .05$), a trend we have previously demonstrated.[4]

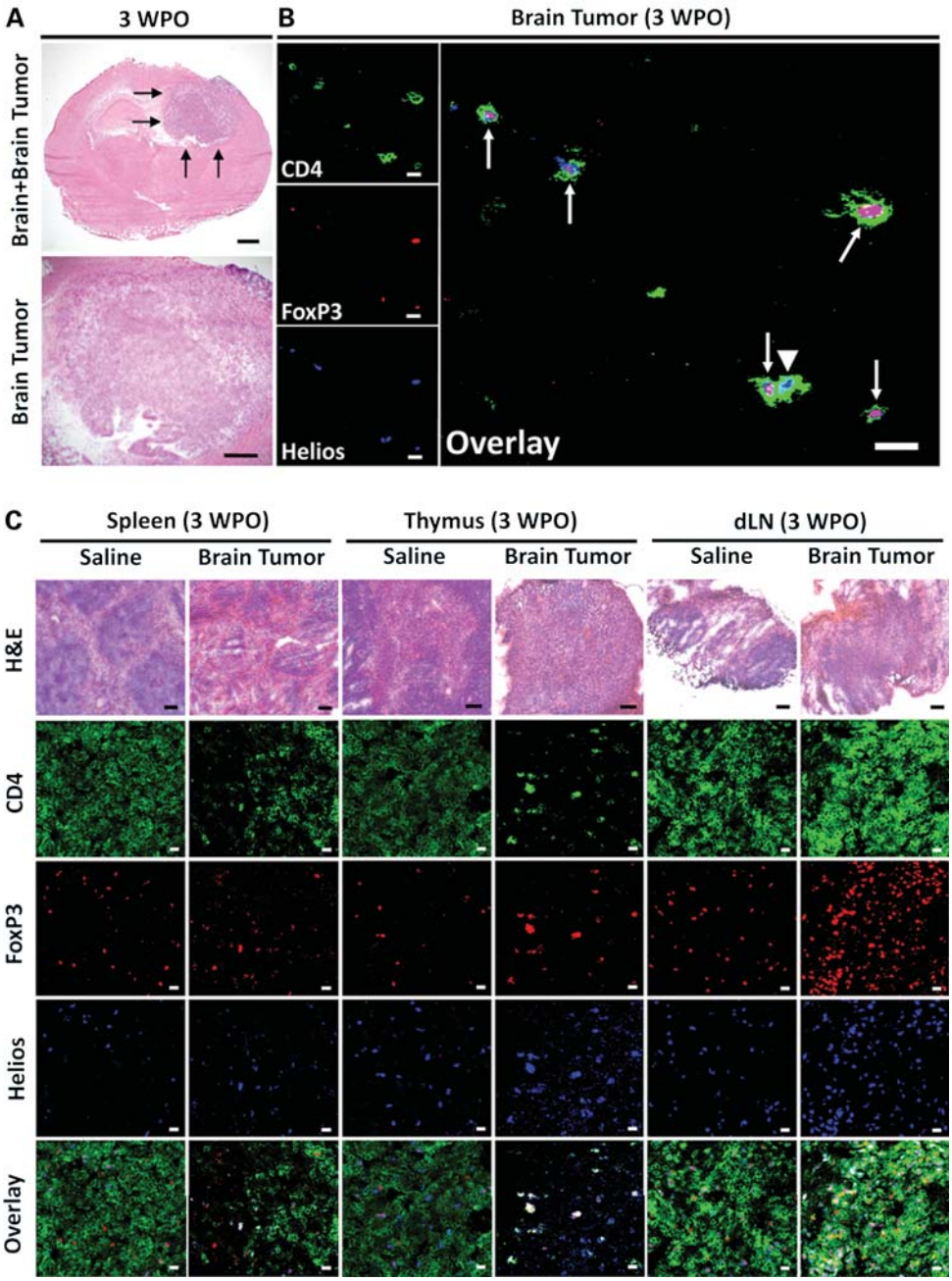

Fig. 5. Anatomical changes occur to secondary immune system structures in mice with GL261 cell-based brain tumors at 3 weeks postoperative (WPO). (A) The mouse brain tumor stains strongly basophilic at 3 WPO. Bars, 1 mm. The 4 black arrows in the upper panel point to the brain tumor. (B) Immunofluorescence in mouse glioma at 3 WPO for CD4 (green), FoxP3 (red), Helios (blue), and an overlay of all 3 signals. Tailed arrows point to $CD4^+$ T cells that are both $FoxP3^+$ and $Helios^+$, while the untailed arrow points to a $CD4^+$ T cell that is $FoxP3^-$ and $Helios^+$. Bars, 25 μm. (C) Spleen, thymus, and cervical draining lymph node (dLN) histology or immunofluorescence for CD4 (green), FoxP3 (red), Helios (blue), and an overlay of all 3 signals between mice i.c. injected with saline or GL261 cells at 3 WPO. Histology bars, 100 μm; immunofluorescence bars, 25 μm. These data were independently repeated in 2 additional mice with similar results.

We analyzed CD103-expressing Tregs and conventional $CD4^+$ T cells, since it has been shown to be increased by Tregs compared with conventional $CD4^+$ T cells.[25] In accordance with the literature, the level of CD103-expressing brain tumor-resident Tregs was higher than brain tumor-resident conventional $CD4^+$ T cells, as well as spleen-derived Tregs and conventional $CD4^+$ T cells ($P < .01$). Also, more spleen-resident Tregs were CD103 positive compared with both brain- and spleen-resident conventional $CD4^+$ T cells ($P < .01$). However, in accordance with what was observed for GITR staining patterns, a higher level of

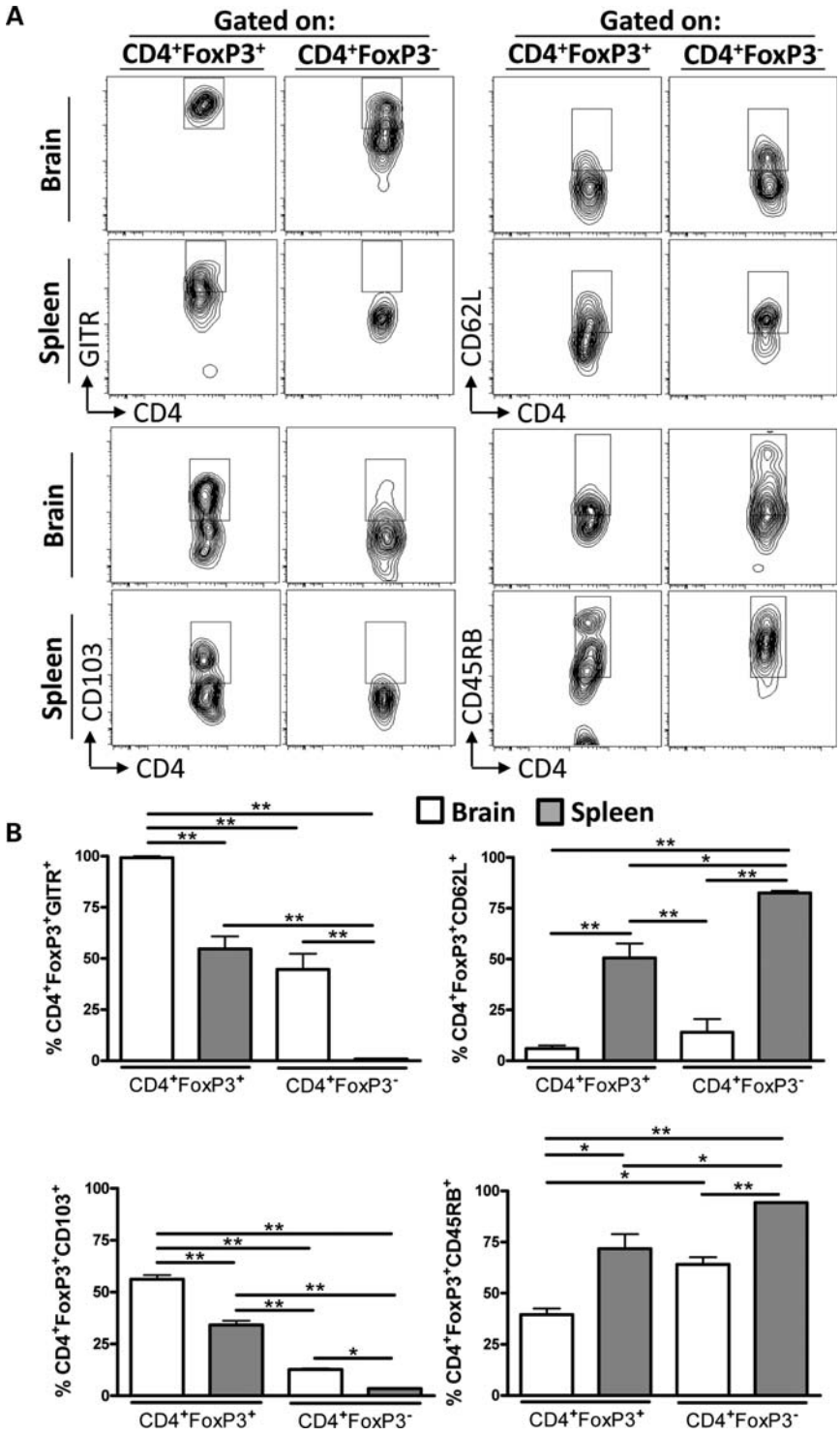

Fig. 6. Brain-resident and splenic Tregs and conventional $CD4^+$ T cells differentially express GITR, CD62L, CD103, and CD45RB in an orthotopic GL261 cell-based mouse brain tumor model at 3-weeks postoperative (WPO). (A) Representative flow cytometry plots of $CD4^+FoxP3^+$ Tregs and conventional $CD4^+$ T cells from brain or spleen that were stained and analyzed for GITR (upper left), CD62L (upper right), CD103 (lower left), and CD45RB (lower right). (B) Quantification of the data based on the gates (from A) for $CD4^+FoxP3^+$ Tregs and conventional $CD4^+$ T cells in the brain (white bars) and spleen (grey bars) at 3 WPO ($n = 3$ per group) coexpressing GITR, CD62L, CD103, and CD45RB. Data in B are shown as mean $\pm$ SEM and are representative of 2 independent experiments. $^*P < .05$, $^{**}P < .01$; n.s., not significant.

brain-resident conventional CD4$^+$ T cells were CD103 positive compared with conventional CD4$^+$ T cells from the spleen ($P < .05$). These data suggest that like GITR, both Tregs and conventional CD4$^+$ T cells are influenced by the brain tumor microenvironment to upregulate CD103.

To confirm the differential expression of markers often associated with differential expression between Tregs and conventional CD4$^+$ T cells, CD45RB expression was analyzed, since it has been shown to be expressed less by Tregs compared with conventional CD4$^+$ T cells.[26] In accordance with the literature, there were fewer CD45RB$^+$ brain-resident Tregs compared with all other groups ($P < .05$). In addition, the level of CD45RB$^+$ spleen-resident Tregs was decreased compared with spleen-resident conventional CD4$^+$ T cells ($P < .05$). Moreover, there was no difference in the level of CD45RB$^+$ spleen-resident Tregs and brain-resident conventional CD4$^+$ T cells. Also, as seen for GITR and CD103, fewer brain-resident conventional CD4$^+$ T cells expressed CD45RB compared with conventional CD4$^+$ T cells in the spleen. Collectively, these data suggest that the tumor microenvironment in the brain has the capability of influencing the developmental program of both Tregs and conventional CD4$^+$ T cells. Specifically, these data suggest that although Tregs are the predominant immunosuppressors, careful consideration of the effects from conventional CD4$^+$ T cells in the context of tumor must also be acknowledged.

nTregs Predominate in GBM

Although both orthotopic and transgenic mouse brain tumor models suggest that Tregs are of a predominantly thymus-derived origin, it is important to establish whether these findings have relevance to human disease. Thus we examined the highly malignant human brain tumor GBM, using a human tissue microarray (Fig. 7A) to count the number of Helios$^+$

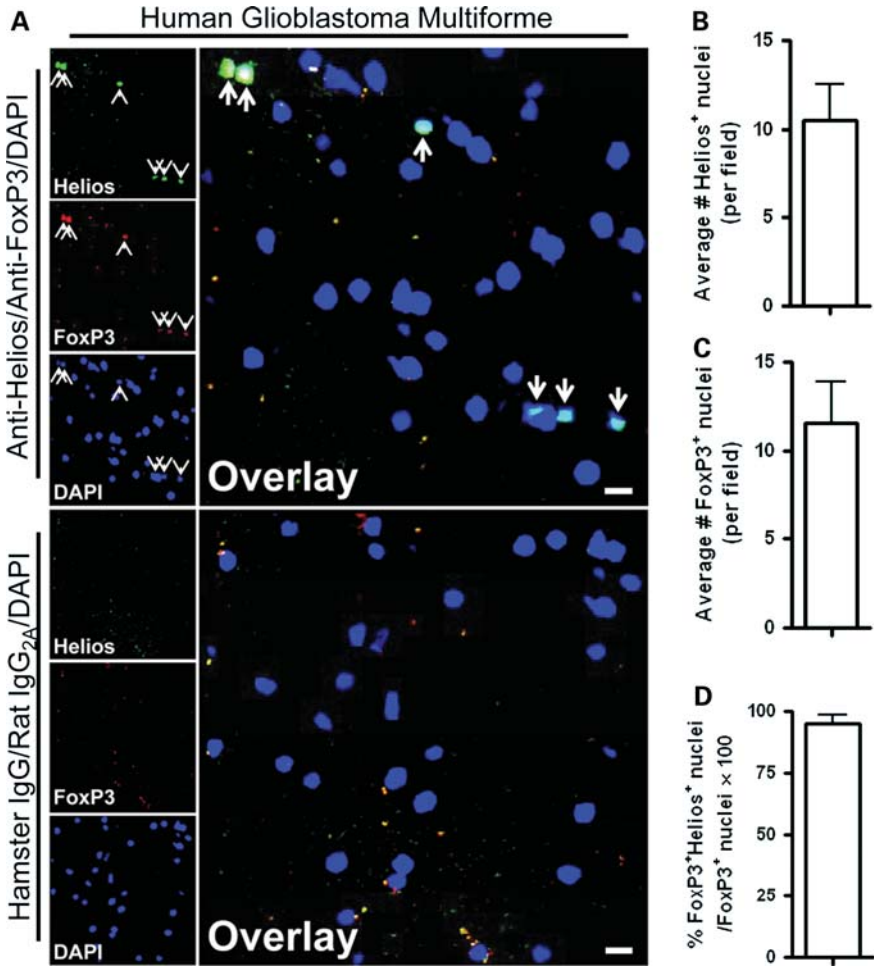

Fig. 7. Thymus-derived Tregs predominate in human glioblastoma multiforme (GBM). (A) A representative immunofluorescence photomicrograph for Helios (green), FoxP3 (red), DAPI (blue), and the overlay, as well as for hamster immunoglobulin (Ig)-G (green), rat IgG_{2A} (red), DAPI (blue), and the overlay in human GBM. Arrows point to nuclei co-stained for FoxP3 and Helios. Bars, 10 μm. The average number of (B) Helios$^+$ and (C) FoxP3$^+$ nuclei were calculated per field of human GBM ($n = 10$ different patient samples). (D) The number of FoxP3$^+$Helios$^+$ coexpressing nuclei was divided by the number of FoxP3$^+$ nuclei and multiplied by 100 to calculate the percentage of thymus-derived Tregs. Data are shown as mean ± SEM.

(Fig. 7B), FoxP3$^+$ (Fig. 7C), and FoxP3$^+$Helios$^+$ coexpressing nuclei (Fig. 7D) in GBM tissue. Similar to our findings in experimental mouse brain tumor models, almost all of the FoxP3$^+$ nuclei that were counted coexpressed the thymus-derived lineage marker, Helios. These data indicate that nTregs constitute the predominant population of Tregs in human GBM.

Discussion

Previous work shows that the conversion of conventional CD4$^+$ T cells into Tregs is the predominant method of replenishment in tumor-bearing mice.[27] The ability of conventional T cells to convert into Tregs is likely due to the expression of TGF-β. It has been demonstrated that high levels of TGF-β result in the conversion of CD4$^+$FoxP3$^-$ T cells into Tregs, which is abrogated with a neutralizing TGF-β antibody.[18] Accordingly, Treg conversion takes place in a mouse model of pancreatic cancer by wild-type conventional CD4$^+$ T cells converting into Tregs, but not by naive conventional CD4$^+$ T cells expressing a dominant negative TGF-β receptor II.[28] In contrast to these reports, recent evidence examining the T-cell receptor repertoire in a carcinogen-induced tumor mouse model has suggested that conventional CD4$^+$ T cells and Tregs do not interconvert,[29] which supports our observations demonstrating that brain tumor-resident Tregs are largely thymus derived and not a result of Treg conversion. Although further study is required to understand the nature of the conflicting reports regarding the origin of tumor-resident Tregs, it is possible that the stroma of the tumor is a critical factor in contributing to whether Tregs are thymus derived or converted from conventional CD4$^+$ T cells. Given the anatomical specialization of the brain, including the presence of the blood-brain barrier (BBB), a difference in the composition of the stroma, and the lack of a conventional lymphatic drainage system,[30] the mechanisms of Treg recruitment in brain tumors may differ from those found in many peripheral environments.

Although the brain tumor is encapsulated in the CNS by the BBB, it causes a systemic response throughout the mouse, as shown by the H&E and immunofluorescence staining in the spleen, thymus, and cervical dLNs. Our analysis at 3 WPO coincides, although it is a fluid process, with signs of weight loss, hunched posture, and a lack of normal physical activity. Furthermore, the smaller size of the follicles in the spleen of brain tumor-bearing mice may be related to the generalized atrophy that occurs throughout the whole animal. Likewise, the cortex-medulla border of the thymus is no longer distinguishable in the thymus at 3 WPO. In contrast, both the high and low cervical dLNs enlarge and become easy to spot during dissection. Part of the reason for the systemic effects of the brain tumor on some of the lymphoid organs in the periphery may be related to the release of endogenous glucocorticoids, since it has been shown that adrenalectomy can partially prevent the apoptosis that leads to the rapid loss of thymocytes.[31] Another possibility is that the direct innervation to lymphoid organs is compromised as a result of brain tumor compression on CNS-resident neurons. It has been well established that the thymus is innervated by neurons in the medulla of the brain as well as in the spinal cord.[32] If projections to the thymus or neurons giving rise to those projections are compromised, it seems reasonable that this would be another mechanism by which thymic atrophy could occur.

Our work tested 2 mouse brain tumor models for the presence of Tregs. The first model was an orthotopic model by which GL261 cells were i.c. implanted. However, this model has intuitively inconvenient drawbacks. Most notably, by virtue of i.c. implantation, the BBB would be at least temporarily damaged and/or destroyed by the surgical drilling of the burr hole through the skull followed by a needle puncturing the dura of the brain. This may be the reason that we observe a low level of detectable CD4$^+$FoxP3$^+$ Tregs in the brain of mice i.c. implanted with saline at 1 WPO. Alternatively, it may be the result of a lack of perfusion prior to harvesting the brain tumor. However, given that Tregs are not detectable in the mouse brain i.c. injected with saline at 3 WPO, we think that the lack of perfusion is unlikely to be the cause of the low level of Treg infiltration. To confirm whether nTregs predominate in a non-orthotopic model, we utilized the spontaneously developing brain tumor, RasB8, transgenic mouse model.[33] The RasB8 mouse model develops low- to high-grade astrocytoma without the need for i.c. injection of glioma cells or cellular transformation by carcinogens. In accordance with what we observed in the orthotopic mouse brain tumor model, Tregs were found to be present in the symptomatic RasB8 mouse brain. Most importantly, the Tregs in the brains of symptomatic RasB8 mice were almost universally thymus derived, as indicated by the coexpression of Helios by CD4$^+$FoxP3$^+$ T cells. More translationally relevant, we confirmed the predominance of thymus-derived Tregs in human GBM via immunofluorescent colocalization of FoxP3 and Helios. Collectively, the data suggest that nTregs predominate in both mouse and human brain tumors.

Since nTregs but not iTregs were the primary resident in brain tumors, we hypothesized that the depletion of nTregs would lead to a significant increase in lifespan. This possibility was tested by thymectomizing mice, with or without the Treg-depleting, CD25 mAb, prior to i.c. implantation of GL261 cells. We were surprised to find that combining thymectomy with CD25 mAb was not as effective in increasing the lifespan of brain tumor-bearing mice as was the administration of CD25 mAb alone. This could be due to the removal of the thymus, which not only participates in nTreg development but also contributes to the development of NK$^+$, conventional CD4$^+$, and CD8$^+$ T cells, all of which have the potential to contribute to tumor eradication.[34,35] Accordingly, recent thymic emigrants of CD8$^+$ T cells are enriched in progressively growing T9 gliomas, further suggesting the

importance of the thymus to contributing to other cells than nTregs during tumor progression.[31] An alternative explanation is that thymectomy primes Tregs for a faster recovery of CD25 expression after CD25 mAb-mediated Treg depletion. It has previously been shown that the systemic administration of CD25 mAb decreases overall CD25 expression on lymphoid cells, which contributes to Treg inactivation.[36] Here, we have confirmed the downregulation and/or loss of CD25 on $CD4^+FoxP3^+$ Tregs after systemic CD25 mAb treatment in vivo (Supplementary Fig. S4). Interestingly, when treated with the CD25 mAb, fewer Tregs in the dLN and ndLN from nontumor bearing unthymectomized mice expressed high levels of CD25 compared with thymectomized mice at 3 WPO. This finding suggests that thymectomy primes Tregs for a faster recovery of high CD25 expression. While we did not study the detailed kinetics of this regulatory mechanism, it is possible that the faster renewal of CD25 on the surface of Tregs in thymectomized mice is associated with a higher level of suppressor function, since CD25 is critical for interleukin-2 signaling and consequent Treg function.[37] If this were true, then it would likely be a contributing factor to the faster time of death of thymectomized mice treated with CD25 mAb compared with unthymectomized mice with brain tumors.

One of the unexpected effects of i.c. injection with saline and/or GL261 cells was the low levels of Tregs in the thymus at 1 WPO followed by an increase in Treg levels at 3 WPO in mice not treated with CD25 mAb. We were unable to find other studies that had analyzed thymic Treg levels at comparable time points in mouse models after injury. While we can only speculate at this time what causes the increase in Treg accumulation in the thymus at the latter time point post-injection, it may be related to injury-associated glucocorticoid signaling or an increase in thymic stromal lymphopoetin and/or keratinocyte growth factor (fibroblast growth factor 7), both of which have been shown to affect Treg development in the thymus.[38–40] It would be interesting to test the effects of adrenalectomy on the injury-associated Treg increase in the thymus. However, to rule out other factors that may be playing a role in Treg development after injury, a global expression analysis comparing factors that govern Treg development between the 1- and 3-WPO time points is planned. Certainly, this could have important implications for future therapies that are not specific to brain tumor burden, but it may also have ramifications for autoimmune-, allergic-, and/or transplant-related pathogenesis.

Although thymus-derived Tregs compose the predominant population in brain tumors, it was interesting to find that they also proliferate at higher levels than iTregs or conventional $CD4^+$ T cells, which was also recapitulated in the dLNs. However, based on our experiments in thymectomy, CD25 mAb, and brain tumor, we propose that nTregs emigrate from the thymus to the dLNs before infiltrating the brain tumor. Thus, it is possible that the higher level of $Ki67^+$ nTregs that was observed both in the dLN and in the brain tumor may simply be a result of expansion in the dLN and remnant expression of Ki67 after transit to the site of the tumor. Furthermore, we believe that the gradual decrease in nTreg levels in the dLN between 1 and 3 WPO occurs as a result of contraction to normal nTreg levels, which has been established to be ~60%.[21] Moreover, recent work has demonstrated the remarkable stability and continuous self-renewal that contributes to the Treg lineage.[41] Our data support this observation and suggest that the population of Tregs that undergo the highest level of self-renewal is thymus derived, since we showed increased levels of $CD4^+FoxP3^+Helios^+$ cells that coexpressed Ki67 compared with $CD4^+FoxP3^+Helios^-$ cells. Furthermore, our data reciprocally support recent work demonstrating an increased level of Tregs that express Ki67 in the tumor infiltrates of primary human breast tumors,[42] as well as work that demonstrates increased intratumoral Treg proliferation in a peripheral mouse tumor model.[43] Thus, the presence of proliferative tumor-resident Tregs appears to extend beyond brain tumors and is likely a feature of both central and peripheral compartmental malignancies, although our data indicate that thymus-derived Tregs are the primary proliferative $CD4^+$ T cell population in brain tumors and dLNs.

Although the Treg developmental program is regulated by FoxP3, genes regulated by FoxP3 demonstrate plasticity depending on the tissue context.[43] Previous work has demonstrated that GITR and CD62L are expressed at higher and lower levels, respectively, on Tregs, while the level of $CD103^+$ Tregs is increased in dLN of tumor-bearing mice, relative to tumor-free mice.[27] Here, we have extended those observations to both Tregs and conventional $CD4^+$ T cells and compared the spleen and brain in tumor-bearing mice. We showed that all of the brain-resident Tregs expressed the co-inhibitory ligand, GITR, while only ~50% of spleen-resident Tregs express it. Interestingly, a significantly increased fraction of brain-resident conventional $CD4^+$ T cells expressed GITR compared with those cells in the spleen. A similar trend was observed for CD103. Likewise, there were fewer CD45RB-expressing Tregs in the brain compared with spleen. Also, fewer conventional $CD4^+$ T cells expressed CD45RB compared with those in the spleen. Collectively, these data suggest that the brain tumor microenvironment amplifies the lineage programming of Tregs. Moreover, conventional $CD4^+$ T cells are also affected by the brain tumor environment, which may be the cause for their recently noted plasticity.

While this is the first report that we know of demonstrating the predominance of nTregs in brain tumors, we plan to revisit other experimental tumor models that have been suggested to consist predominantly of iTregs, to confirm their origin, the comparative numbers of Tregs expressing GITR, CD62L, CD103, and CD45RB, as well as the proliferative status. It would be interesting to find that the tumor

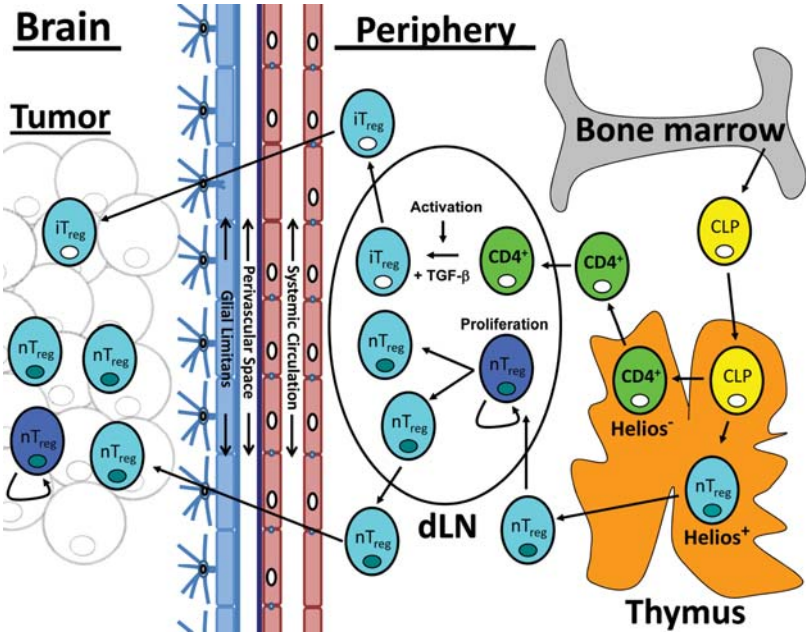

Fig. 8. Model of Treg recruitment in brain tumors. Common lymphoid progenitor (CLP) cells develop in the bone marrow and migrate to the thymus. In the thymus, CLP cells can terminally differentiate into naive conventional CD4$^+$ T cells (light green cell : white nucleus) or mature thymus-derived natural Tregs (nTregs) that coexpress FoxP3 and Helios (light blue cell : dark blue nucleus). Both conventional CD4$^+$ T cells and mature nTregs emigrate from the thymus and are home to cervical tumor draining lymph nodes (dLNs). In the dLN, conventional CD4$^+$ T cells undergo activation and, when in the presence of TGF-β, differentiate into inducible Tregs (iTregs). In contrast, nTregs undergo an early expansion (as shown by Ki67 expression). The iTregs and nTregs then emigrate from the dLN, where they are differentially recruited to the brain tumor. Both mature nTregs and activated iTregs can then enter the systemic circulatory system, where they are differentially recruited to the brain tumor by crossing both the perivascular space and glial limitans, before entering the brain tumor parenchyma. While nTregs are preferentially recruited, iTregs rarely migrate into the brain tumor. At the site of the brain tumor, nTregs undergo a low but detectable level of proliferation (as shown by Ki67 expression).

microenvironment within the CNS programmed Tregs differently than in subcutaneous tumor models in the peripheral nervous system. Already we have shown that a distinct subset of brain-resident Tregs, in vivo, coexpress the pro-inflammatory cytokine interleukin-17A.[44] This is a surprising finding given that almost all of the brain tumor-resident Tregs are nTregs and previous data demonstrating the cytokine-producing stability of nTregs when compared with iTregs.[21] However, it is important to point out that the conditions by which cytokine production occurs in nTregs and iTregs in vitro are unlikely to be recapitulated by the tumor microenvironment. To confirm this suggestion, we are currently engaged in tracking the stability of nTreg conversion in vivo utilizing FoxP3–interleukin-17 coreporter mice.

In summary, this work identifies that the thymus-derived nTreg is the predominant type of Treg in human GBM and experimental mouse brain tumors. A working model describing our data in the context of the current literature is presented in Figure 8. Functionally, we tested the relevance of nTregs in a mouse brain tumor model, using thymectomy and CD25 mAb and found that the thymus is critical for the beneficial effects of CD25 mAb. Furthermore, more brain-resident Tregs express GITR and CD103 compared with spleen-resident Tregs in tumor-bearing mice. In contrast, fewer brain-resident Tregs express CD62L and CD45RB compared with spleen-resident Tregs in tumor-bearing mice. Finally, we showed that more nTregs express Ki67 in the brain and cervical dLNs compared with iTregs and conventional CD4$^+$ T cells. While most of the data that we have presented here are representative of the Treg origin in a mouse brain tumor model, we believe that these data have implications for the clinical treatment of GBM, given that we confirmed that nTregs predominate in human GBM. First, Tregs will need to be targeted in the periphery, where nTreg development and expansion predominates. Likewise, Tregs may need to be targeted in the brain, since brain tumor patients will present with Tregs already infiltrating the malignancy, in addition to the proliferative status. This will require chemotherapeutics and/or immunotherapeutic modalities that are capable of freely passing through the BBB, as well as targeting both proliferating tumor cells and nTregs. Coincidentally, these studies are currently ongoing in a clinical trial, NCT00626483, which is testing the combined efficacy of temozolomide and daclizumab in patients with GBM. The therapeutic effect of temozolomide depends on the ability to alkylate/methylate DNA, triggering tumor

cell death, while daclizumab is a humanized anti–interleukin-2 receptor antibody. Our data support the rationale for this combinatorial strategy as well as the development of future strategies whereby both reagents readily cross the BBB.

Supplementary Material

Supplementary material is available online at *Neuro-Oncology* (http://neuro-oncology.oxfordjournals.org/).

Acknowledgments

We thank Feifei Liu for expertise in statistically analyzing the data.

Conflict of interest statement. None declared.

Funding

This work was supported by NIH grant R01CA138587 (M.S.L.) and NIH grant F32NS073366 (D.A.W.).

References

1. Stupp R, Mason WP, van den Bent MJ, et al. Radiotherapy plus concomitant and adjuvant temozolomide for glioblastoma. *N Engl J Med*. 2005;352:987–996.
2. Pellegatta S, Poliani PL, Stucchi E, et al. Intra-tumoral dendritic cells increase efficacy of peripheral vaccination by modulation of glioma microenvironment. *Neuro Oncol*. 2010;12:377–388.
3. Curtin JF, Liu N, Candolfi M, et al. HMGB1 mediates endogenous TLR2 activation and brain tumor regression. *PLoS Med*. 2009;6:e10.
4. El Andaloussi A, Han Y, Lesniak MS. Prolongation of survival following depletion of CD4+CD25+ regulatory T cells in mice with experimental brain tumors. *J Neurosurg*. 2006;105:430–437.
5. Yu JS, Burwick JA, Dranoff G, et al. Gene therapy for metastatic brain tumors by vaccination with granulocyte-macrophage colony-stimulating factor-transduced tumor cells. *Hum Gene Ther*. 1997;8:1065–1072.
6. El Andaloussi A, Lesniak MS. An increase in CD4+CD25+FOXP3+ regulatory T cells in tumor-infiltrating lymphocytes of human glioblastoma multiforme. *Neuro Oncol*. 2006;8:234–243.
7. El Andaloussi A, Lesniak MS. CD4+ CD25+ FoxP3+ T-cell infiltration and heme oxygenase-1 expression correlate with tumor grade in human gliomas. *J Neurooncol*. 2007;83:145–152.
8. Heimberger AB, Abou-Ghazal M, Reina-Ortiz C, et al. Incidence and prognostic impact of FoxP3+ regulatory T cells in human gliomas. *Clin Cancer Res*. 2008;14:5166–5172.
9. Fecci PE, Mitchell DA, Whitesides JF, et al. Increased regulatory T-cell fraction amidst a diminished CD4 compartment explains cellular immune defects in patients with malignant glioma. *Cancer Res*. 2006;66:3294–3302.
10. Curtin JF, Candolfi M, Fakhouri TM, et al. Treg depletion inhibits efficacy of cancer immunotherapy: implications for clinical trials. *PLoS One*. 2008;3:e1983.
11. Shimizu J, Yamazaki S, Takahashi T, et al. Stimulation of CD25(+)CD4(+) regulatory T cells through GITR breaks immunological self-tolerance. *Nat Immunol*. 2002;3:135–142.
12. Read S, Malmström V, Powrie F. Cytotoxic T lymphocyte–associated antigen 4 plays an essential role in the function of CD25(+)CD4(+) regulatory cells that control intestinal inflammation. *J Exp Med*. 2000;192:295–302.
13. Zheng SG, Wang JH, Gray JD, et al. Natural and induced CD4+CD25+ cells educate CD4+CD25- cells to develop suppressive activity: the role of IL-2, TGF-beta, and IL-10. *J Immunol*. 2004;172:5213–5221.
14. Hsieh CS, Zheng Y, Liang Y, et al. An intersection between the self-reactive regulatory and nonregulatory T cell receptor repertoires. *Nat Immunol*. 2006;7:401–410.
15. Wong J, Obst R, Correia-Neves M, et al. Adaptation of TCR repertoires to self-peptides in regulatory and nonregulatory CD4+ T cells. *J Immunol*. 2007;178:7032–7041.
16. Hori S, Nomura T, Sakaguchi S. Control of regulatory T cell development by the transcription factor Foxp3. *Science*. 2003;299:1057–1061.
17. Jordan MS, Boesteanu A, Reed AJ, et al. Thymic selection of CD4+CD25+ regulatory T cells induced by an agonist self-peptide. *Nat Immunol*. 2001;2:301–306.
18. Liu VC, Wong LY, Jang T, et al. Tumor evasion of the immune system by converting CD4+CD25- T cells into CD4+CD25+ T regulatory cells: role of tumor-derived TGF-beta. *J Immunol*. 2007;178:2883–2892.
19. Kretschmer K, Apostolou I, Hawiger D, et al. Inducing and expanding regulatory T cell populations by foreign antigen. *Nat Immunol*. 2005;6:1219–1227.
20. Zhou G, Levitsky HI. Natural regulatory T cells and de novo–induced regulatory T cells contribute independently to tumor-specific tolerance. *J Immunol*. 2007;178:2155–2162.
21. Thornton AM, Korty PE, Tran DQ, et al. Expression of Helios, an Ikaros transcription factor family member, differentiates thymic-derived from peripherally induced Foxp3+ T regulatory cells. *J Immunol*. 2010;184:3433–3441.
22. Ding H, Roncari L, Shannon P, et al. Astrocyte-specific expression of activated p21-ras results in malignant astrocytoma formation in a transgenic mouse model of human gliomas. *Cancer Res*. 2001;61:3826–3836.
23. Malizia G, Trejdosiewicz LK, Wood GM, et al. The microenvironment of coeliac disease: T cell phenotypes and expression of the T2 'T blast' antigen by small bowel lymphocytes. *Clin Exp Immunol*. 1985;60:437–446.
24. McHugh RS, Whitters MJ, Piccirillo CA, et al. CD4+CD25+ immunoregulatory T cells: gene expression analysis reveals a functional role for the glucocorticoid-induced TNF receptor. *Immunity*. 2002;16:311–323.
25. Rao PE, Petrone AL, Ponath PD. Differentiation and expansion of T cells with regulatory function from human peripheral lymphocytes by stimulation in the presence of TGF-β. *J Immunol*. 2005;174:1446–1455.
26. Chen W, Jin W, Hardegen N, et al. Conversion of peripheral CD4+CD25- naive T cells to CD4+CD25+ regulatory T cells by TGF-beta induction of transcription factor Foxp3. *J Exp Med*. 2003;198:1875–1886.

27. Valzasina B, Piconese S, Guiducci C, et al. Tumor-induced expansion of regulatory T cells by conversion of CD4+CD25 lymphocytes is thymus and proliferation independent. *Cancer Res*. 2006;66: 4488–4495.
28. Moo-Young TA, Larson JW, Belt BA, et al. Tumor-derived TGF-beta mediates conversion of CD4+Foxp3+ regulatory T cells in a murine model of pancreas cancer. *J Immunother*. 2009;32:12–21.
29. Hindley JP, Ferreira C, Jones E, et al. Analysis of the T-cell receptor repertoires of tumor-infiltrating conventional and regulatory T cells reveals no evidence for conversion in carcinogen-induced tumors. *Cancer Res*. 2011;71:736–746.
30. Weller RO, Djuanda E, Yow HY, et al. Lymphatic drainage of the brain and the pathophysiology of neurological disease. *Acta Neuropathol*. 2009;117:1–14.
31. Prins RM, Graf MR, Merchant RE, et al. Thymic function and output of recent thymic emigrant T cells during intracranial glioma progression. *J Neurooncol*. 2003;64:45–54.
32. Bulloch K, Moore RY. Innervation of the thymus gland by brain stem and spinal cord in mouse and rat. *Am J Anat*. 1981;162:157–166.
33. Shannon P, Sabha N, Lau N, et al. Pathological and molecular progression of astrocytomas in a GFAP:12 V-Ha-Ras mouse astrocytoma model. *Am J Pathol*. 2005;167:859–867.
34. Yamasaki K, Horiguchi S, Kurosaki M, et al. Induction of NKT cell-specific immune responses in cancer tissues after NKT cell-targeted adoptive immunotherapy. *Clin Immunol*. 2011;138:255–265.
35. Schietinger A, Philip M, Liu RB, et al. Bystander killing of cancer requires the cooperation of CD4(+) and CD8(+) T cells during the effector phase. *J Exp Med*. 2010;207:2469–2477.
36. Kohm AP, McMahon JS, Podojil JR, et al. Cutting edge: anti-CD25 monoclonal antibody injection results in the functional inactivation, not depletion, of CD4+CD25+ T regulatory cells. *J Immunol*. 2006;176:3301–3305.
37. Barron L, Dooms H, Hoyer KK, et al. Cutting edge: mechanisms of IL-2-dependent maintenance of functional regulatory T cells. *J Immunol*. 2010;185:6426–6430.
38. Jiang Q, Su H, Knudsen G, et al. Delayed functional maturation of natural regulatory T cells in the medulla of postnatal thymus: role of TSLP. *BMC Immunol*. 2006;7:6.
39. Mazzucchelli R, Hixon JA, Spolski R, et al. Development of regulatory T cells requires IL-7Ralpha stimulation by IL-7 or TSLP. *Blood*. 2008;112:3283–3292.
40. Bruinsma M, van Soest PL, Leenen PJ, et al. Keratinocyte growth factor induces expansion of murine peripheral CD4+Foxp3+ regulatory T cells and increases their thymic output. *J Immunol*. 2007;179:7424–7430.
41. Rubtsov YP, Niec RE, Josefowicz S, et al. Stability of the regulatory T cell lineage in vivo. *Science*. 2010;329:1667–1671.
42. Gobert M, Treilleux I, Bendriss-Vermare N, et al. Regulatory T cells recruited through CCL22/CCR4 are selectively activated in lymphoid infiltrates surrounding primary breast tumors and lead to an adverse clinical outcome. *Cancer Res*. 2009;69:2000–2009.
43. Lutsiak ME, Tagaya Y, Adams AJ, et al. Tumor-induced impairment of TCR signaling results in compromised functionality of tumor-infiltrating regulatory T cells. *J Immunol*. 2008;180:5871–5878.
44. Wainwright DA, Sengupta S, Han Y, et al. The presence of IL-17A and T helper 17 cells in experimental mouse brain tumors and human glioma. *PLoS One*. 2010;5:e15390.